Tellus (2005), 57A, 194–203
Printed in UK. All rights reserved

TELLUS

Estimation of Spatial Global Positioning System Zenith Delay observation error covariance

By REIMA ERESMAA and HEIKKI JÄRVINEN*, [1]*Finnish Meteorological Institute, Vuorikatu 24, FIN-00100 Helsinki, Finland*

(Manuscript received 31 March 2004; in final form 13 September 2004)

ABSTRACT

In this paper, we present new methods and estimates of the spatial (horizontal) covariance of the ground-based Global Positioning System Zenith Delay observation errors. An algorithm is developed which enables estimation of the observation error covariance as a linear combination of innovation covariances of Zenith Total Delay (ZTD) at ground-based receiver stations, surface pressure at synoptic stations and integrated water vapour at radiosonde stations, respectively. Innovation (observation minus model background) sequences computed with the High-Resolution Limited Area Model (HIRLAM) are used as statistical material for the estimation. We present a four-parameter exponential observation error covariance model for the ZTD horizontal observation error covariance. Seasonal and yearly mean models are provided for implementation into meteorological data assimilation systems.

1. Introduction

Data assimilation blends observations and model background in a statistically optimal way. Optimality requires accurate estimation of the observation and background error statistics. Data assimilation methods allow specification of observation error covariance but the practical implementations favour observation types with uncorrelated errors. Typically, balloon soundings, for instance, are mutually independent and thus have uncorrelated observation errors, apart from certain systematic instrumental biases, such as radiative warming of the sonde in the stratosphere. Generally speaking, *in situ* observation errors are spatially uncorrelated whereas remote sensing measurement errors are spatially correlated. Furthermore, observation errors of *in situ* and remote sensing data can be temporally correlated, which poses an additional complication for data assimilation (Järvinen et al., 1999). Estimation of these spatial and temporal observation error correlations is similarly impeded as there is no general method available for separation of observation and background error contributions to the innovation (observation minus model background) covariance.

There are several sources of spatial observation error covariance related to remote sensing data. An obvious source is built into the observing system philosophy: the same instrument is used for producing a large number of observations, and therefore instrumental errors are replicated into each new piece of information. These errors may appear as observation-type specific biases and it may be possible to detect and correct them. Another less obvious source of spatial observation error covariance is observation preprocessing and retrieval methodology. Preprocessing, such as satellite image navigation, is always part of the processing chain of remote sensing data, although in data assimilation as little preprocessing as possible is usually preferred. More importantly, climatology or background information can be used to constrain the inversion (or retrieval) of measured quantities into geophysical quantities. The spatially correlated background (or climatology) errors are thus included into the inversion solution and all measurements generated by the inversion can be affected. Description and interpretation of these error patterns can be difficult.

It is desirable from the data assimilation point of view to have observing systems with uncorrelated observation errors. Uncorrelated observation errors lead to relatively simple computation of the observation contribution to the analysis increment. A properly implemented observation error covariance model increases the complexity of the computational code of the data assimilation system where scalar algebra of diagonal observation error covariance matrices is replaced by vector algebra of non-diagonal observation error covariance matrices.

Observation error correlation implies a reduced information content of the observations due to information redundancy. If correlated observation errors are not properly accounted for, an overly large weight is given for this source of information. Weak observation error correlations are often dealt with using ad hoc methods, rather than through proper error estimation, error

*Corresponding author.
e-mail: heikki.jarvinen@fmi.fi

modelling and assimilation code modification. Perhaps the most commonly used ad hoc method is data thinning, which means using original data with reduced spatial (and temporal) resolution. This approach is justified if the observation error covariance length-scale is short compared with the resolution of the thinned data. Another simple ad hoc method is the reduction of observation weight in data assimilation by artificially increasing the specified observation error variance. This approach must be regarded as a temporary fix to alleviate problems associated with non-modelled observation error covariance. The proper solution is to estimate, model and implement the observation error covariance into the data assimilation system.

Finally, one should perhaps bear in mind that for the optimality of the data assimilation system, it is essential to accurately estimate and model the spatial structures of the background error covariance. Spatial structure of the observation error covariance is important to account for, but the actual functional form of the observation error covariance is much less critical for the optimality of the data assimilation system than is the spatial structure of the background error covariance.

The High-Resolution Limited Area Model (HIRLAM; Undén et al., 2002), together with the HIRLAM three-dimensional variational data assimilation system (Gustafsson et al., 2001; Lindskog et al., 2001), is the operational numerical weather prediction (NWP) system of several European National Meteorological Services. The HIRLAM community is making an effort to assimilate Global Positioning System (GPS) Zenith Total Delay (ZTD) observations. ZTD observations are known to suffer from complex error structures including significant station-dependent biases and horizontal observation error covariance (Haase et al., 2003; Stoew, 2004), which are not specified in the HIRLAM data assimilation system. Reported ZTD data assimilation experiments also lack spatial observation error covariance modelling (e.g. De Pondeca and Zou, 2001; Gustafsson, 2002).

A method for estimating the spatial ZTD observation error covariance is presented in this paper. It is based on the observation method for background error covariance estimation (Hollingsworth and Lönnberg, 1986, hereafter HL86). A textbook treatment of the observation method can be found in Daley (1991) or Bouttier and Courtier (1999). Because the observation method assumes spatially uncorrelated observation errors, it is not directly applicable for estimation of ZTD background and observation error covariances. This study applies the observation method to obtain the spatial innovation covariance estimates for ZTD, surface pressure (p_s) and Integrated Water Vapour (IWV) using data from ground-based GPS receivers, synoptic stations and radiosonde stations, respectively. With certain decorrelation assumptions of the conventional observation and model field errors, the spatial ZTD observation error covariance can be estimated as a linear combination of the estimated innovation covariances.

This paper is structured as follows. In Section 2 we describe ZTD error characteristics and the error covariance estimation and modelling approach, in Section 3 we reveal the developed innovation covariance models for ZTD, p_s and IWV, and in Section 4 we present the seasonal four-parameter spatial (horizontal) ZTD observation error covariance model. Finally, results are discussed in Section 5.

2. Observations and methods

2.1. Global Positioning System network solution

GPS is primarily a non-meteorological satellite system, which can be used to produce meteorological observations by applying a preprocessing and retrieval technique (Bevis et al., 1992).

The GPS system consists of a number of satellites broadcasting microwave signals, which are received by a network of ground-based receivers. Signal phase information can be used to estimate satellite and receiver positions and their clock errors as a solution of a simultaneous least-squares (L-S) estimation problem. ZTD is estimated for each receiver as one network solution parameter. Geodetic use of ZTD in the network solution is to map ZTD from the zenith direction to all different spatial directions related to signals from different satellites.

The ZTD observation error can contain contributions from uncertainties in any component of the network: satellite and receiver position and clock errors as well as errors in the mapping procedure. These errors are propagated across the network solution in the L-S estimation procedure. As discussed in the introduction, this preprocessing and retrieval methodology contains the ingredients for generating spatially correlated ZTD observation errors.

2.2. Zenith Total Delay observations

The atmosphere affects electromagnetic GPS signals by retarding their propagation speed through the neutral refractivity of air (N). In the GPS literature, this phenomenon is called the tropospheric refraction, which along a signal path s is defined by an integral

$$\Delta^{\mathrm{Trop}} = 10^{-6} \int_s N \mathrm{d}s, \tag{1}$$

$$N = k_1 \frac{p_\mathrm{d}}{T} + k_2 \frac{e}{T} + k_3 \frac{e}{T^2}, \tag{2}$$

where p_d and e are partial pressures of dry air and water vapour, respectively, T is temperature and k_1, k_2 and k_3 are the refractivity coefficients (Bevis et al., 1992). Integration of eq. (1) along the local vertical from the ground level to the top of the atmosphere results in Δ^{Trop} equal to ZTD. ZTD is expressed in units of length and its magnitude in standard atmospheric conditions is around 2.5 m.

It is a common practice to separate ZTD into Zenith Hydrostatic Delay (ZHD) and Zenith Wet Delay (ZWD; Saastamoinen,

1972; Bevis et al., 1992). In typical atmospheric conditions, ZHD contributes about 90% of ZTD and it depends on altitude, latitude and atmospheric pressure. It is adequate to have measurements of p_s only in order to estimate ZHD. However, the meteorological interest of ZTD is primarily due to ZWD, which depends on the vertical distributions of temperature and water vapour above the receiver and thus cannot be accurately estimated by surface measurements alone. ZWD is proportional to IWV, and the factor of proportionality depends on the local atmospheric temperature and humidity profiles.

A simplified notation

$$\mathrm{ZTD} = \mathrm{ZHD} + \mathrm{ZWD} = ap_s + b\mathrm{IWV} \tag{3}$$

is used here. The coefficients a and b are treated as constants and they are calculated by assuming receiver located at the latitude 45°N at the mean sea level, and the standard subarctic summer vertical distributions of temperature and humidity (McClatchey et al., 1971) are used. These assumptions lead to coefficient values $a = 2.2809$ mm hPa^{-1} and $b = 6.2777$.

2.3. Zenith Total Delay errors and innovation covariances

Innovation d, in Kalman filter terminology, is defined as observation minus model counterpart calculated from the background state vector. ZTD innovation d_{ZTD} is equal to observed minus background ZTD or, equivalently, to ZTD observation error $\varepsilon^{\mathrm{o}}_{\mathrm{ZTD}}$ minus ZTD background error $\varepsilon^{\mathrm{b}}_{\mathrm{ZTD}}$ (see Appendix A). Using eq. (3), $\varepsilon^{\mathrm{b}}_{\mathrm{ZTD}}$ and d_{ZTD} can be written as

$$\varepsilon^{\mathrm{b}}_{\mathrm{ZTD}} = a\varepsilon^{\mathrm{b}}_{p_s} + b\varepsilon^{\mathrm{b}}_{\mathrm{IWV}}$$
$$d_{\mathrm{ZTD}} = \varepsilon^{\mathrm{o}}_{\mathrm{ZTD}} - \varepsilon^{\mathrm{b}}_{\mathrm{ZTD}} = \varepsilon^{\mathrm{o}}_{\mathrm{ZTD}} - a\varepsilon^{\mathrm{b}}_{p_s} - b\varepsilon^{\mathrm{b}}_{\mathrm{IWV}},$$

where $\varepsilon^{\mathrm{b}}_{p_s}$ and $\varepsilon^{\mathrm{b}}_{\mathrm{IWV}}$ are p_s and IWV background errors, respectively.

Because d_{ZTD} is a sum of three terms, there are nine terms contributing to the ZTD innovation covariance (see Appendix A). After certain error decorrelation assumptions, the spatial covariance of two ZTD innovation sequences $d_{\mathrm{ZTD},i}$ and $d_{\mathrm{ZTD},j}$ from stations i and j can be formulated as eq. (A1) of Appendix A

$$\underbrace{\mathrm{cov}(d_{\mathrm{ZTD},i}, d_{\mathrm{ZTD},j})}_{\text{INN term}} = \underbrace{\mathrm{cov}(\varepsilon^{\mathrm{o}}_{\mathrm{ZTD,i}}, \varepsilon^{\mathrm{o}}_{\mathrm{ZTD},j})}_{\text{OBS term}} + \underbrace{a^2\mathrm{cov}(d_{p_s,i}, d_{p_s,j})}_{\text{ZHD term}} + \underbrace{b^2\mathrm{cov}(d_{\mathrm{IWV},i}, d_{\mathrm{IWV},j})}_{\text{ZWD term}}. \tag{4}$$

The covariance of the ZTD observation error ($\varepsilon^{\mathrm{o}}_{\mathrm{ZTD}}$; OBS term) is unknown while the covariances of the ZTD innovation (d_{ZTD}; INN term), p_s innovation (d_{p_s}; ZHD term) and IWV innovation (d_{IWV}; ZWD term) can be estimated from innovation sequences of ZTD at ground-based receiver stations, p_s at synoptic surface stations and IWV at radiosonde stations, respectively. In summary, the task is to estimate the three innovation covariance terms of eq. (4) and their linear combination is the unknown ZTD observation error covariance.

2.4. Innovation covariance modelling

The observation method is applied here for estimating the spatial innovation covariance terms of eq. (4). HL86 tuned the spatial covariance structure of the background errors of the European Centre for Medium-Range Weather Forecasts (ECMWF) Optimum Interpolation system with bias-corrected radiosonde data. These observations have spatially (horizontally) uncorrelated errors and the estimation of observation error variance and background error covariance is straightforward. For this study, HL86 provide the methodological framework for the innovation covariance estimation.

In the observation method, all possible station pairs at each analysis time are formed and these pairs are classified into bins according to the station separation. Innovation covariance is calculated for all bins of station separation and a covariance model is L-S fitted to the bin-averaged covariance values. HL86 fitted a Bessel series, while a simpler exponential function is used here. 95% confidence intervals are also calculated for each bin-averaged covariance value and the inverses of these widths are used as weighting in the L-S fitting procedure.

The innovation covariance is modelled in this study by a serial exponential function

$$f(r) = \sum_{i=1}^{N} R_i \left(1 + \frac{r}{L_i}\right) \exp\left(-\frac{r}{L_i}\right). \tag{5}$$

This covariance model is a generalized version of that introduced in the case $N = 1$ by Thiébaux (1985) and later used by, for example, Daley (1991) and Bormann et al. (2003).

The covariance model (5) is defined by estimating the parameters R_i and L_i. The model (5) is only a function of separation distance r, which implies that horizontally homogeneous and isotropic error covariance is assumed. Provided that the parameter values are positive, the covariance model (5) has the following properties. First, the model values $f(r)$ decrease with increasing r. Secondly,

$$\left.\frac{\partial f}{\partial r}\right|_{r=0} = 0 \quad \text{and} \quad \left.\frac{\partial f}{\partial r}\right|_{r=\infty} = 0.$$

Thirdly, the resulting error covariance matrix is positive definite, and thus invertible.

In this paper we apply $N = 2$ in eq. (5) which equals a four-parameter covariance model

$$f(r) = R_1 \left(1 + \frac{r}{L_1}\right) \exp\left(-\frac{r}{L_1}\right) + R_2 \left(1 + \frac{r}{L_2}\right) \exp\left(-\frac{r}{L_2}\right). \tag{6}$$

2.5. *Practical approaches for observation error covariance model estimation*

Fitting the covariance model to data involves model parameter estimation which can be constrained by either the L-S or the maximum-likelihood (M-L) principles. In this study, the procedure of HL86 is followed and the parameter estimation is thus based on the L-S method. A theoretical description of the M-L method can be found, for example, in Dee and da Silva (1999) with applications in Dee et al. (1999).

There are, in practice, two alternative approaches with different implementation details for L-S estimation of the model parameters. These approaches will be called 'estimation in model space' and 'estimation in innovation space'. As will be seen later, both approaches result in fairly similar results.

The first approach (estimation in model space) is to fit a separate $N = 2$ model for each of the three innovation terms of eq. (4). The model for the OBS term is then obtained by subtracting the ZHD model and the ZWD model from the INN model. The resulting OBS model will be a $N = 6$ model. For this model, all parameter values are not positive, and the properties of eq. (5) required from a proper covariance model are not valid. Therefore, a reduction back to a $N = 2$ model is necessary. The reduction procedure is as follows. The $N = 6$ model is applied to generate covariance values with sufficient spacing for the whole separation distance range. Reduction is then carried out by fitting a $N = 2$ model to this data set. A spacing of 1 km is used here for the range of up to 2000 km, but a spacing of up to a few tens of kilometres is found to be sufficient for obtaining stable estimates of the $N = 2$ model parameters. Uniform weighting is used in this L-S fitting.

The second approach (estimation in innovation space) is to calculate the bin-averaged innovation covariance values with exactly the same separation distances and bin widths for all three terms of eq. (4). Bin-averaged innovation covariance values for ZHD and ZWD are then subtracted from the INN values, and the $N = 2$ OBS model is L-S fitted to these binned residual covariance values.

In the first approach, different bin widths can be chosen for the estimation of different terms of eq. (4) as the separation is performed in the covariance model space. The model fitting also poses additional filtering on the bin-averaged innovation covariance values. In the second approach, on the other hand, there are fewer estimation steps, and less data filtering. There is also a constraint for using exactly the same binning for each innovation data type and the most sparse innovation data type dictates the binning details.

3. Innovation covariance modelling

In this section, an $N = 2$ model is fitted to the bin-averaged covariance values for ZTD, p_s and IWV innovations, respectively. The model parameters are estimated for the standard three-month seasons and for the yearly mean covariances. Monthly model parameter estimates are noisy and are not discussed here.

3.1. *Zenith Total Delay innovation covariance*

ZTD innovation covariance (INN term of eq. 4) is estimated using the following data set. ZTD observations are post-processed by the Chalmers Technical University, Onsala Observatory, Sweden and the model counterparts are computed with the 22-km resolution operational HIRLAM NWP system at the Swedish Meteorological and Hydrological Institute (SMHI). The data set consists of ZTD innovations for a 1-yr period from May 2000 to April 2001 for 35 Finnish and Swedish ground-based GPS stations.

The SMHI innovation data set enables estimation of the covariance for station separation distances of 50–1500 km. In order to minimize the effects of biases in the estimation of covariance, monthly biases are calculated for all GPS receiving stations and all analysis times (00, 06, 12 and 18 UTC). The station and analysis time-dependent monthly biases range from −24.3 to 32.9 mm ZTD, where a positive value indicates background ZTD being systematically higher than observed ZTD. The mean bias of the data set is −7.1 mm.

The covariance is calculated from the bias-corrected innovations with classification into 100-km separation distance bins. Figure 1 shows an example of ZTD innovation covariance for the autumn period (three months of data). The bin-averaged covariance values and their 95% confidence intervals are denoted by dots and the vertical bars, respectively. The solid curve shows the fitted covariance model for the spatially correlated part of the innovation. According to HL86, the zero separation covariance value contains a contribution from the uncorrelated part of the innovation and is therefore not used in the fitting procedure. An investigation of Fig. 1, and of similar figures for other seasons (not shown), supports the following conclusions. First, the

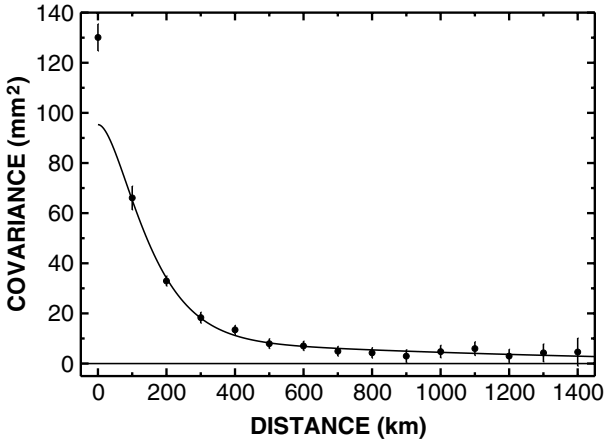

Fig 1. GPS ZTD innovation covariance model for the three-month autumn period, i.e. an estimate of the INN term of eq. (4).

covariance model is able to closely fit the bin-averaged ZTD innovation covariance values. Secondly, with increasing separation distance r, the ZTD innovation covariance decreases rapidly, and the e-folding distance is about 200 km. Thirdly, ZTD innovation covariance does not asymptotically approach zero with increasing separation distance r. These large-scale covariance structures appear in the three-month periods for autumn (Fig. 1) and winter (not shown) but not for spring or summer. Finally, the ZTD innovation covariance at short separation distances, as well as the ZTD innovation variance (i.e. innovation covariance at zero separation), has a clear annual cycle with a maximum in summer and a minimum in winter, and with autumn and spring values symmetrically in between. This annual cycle coincides with the annual cycle of the atmospheric moisture content at northern mid-latitudes.

3.2. p_s innovation covariance

Innovation covariance for p_s (the ZHD term of eq. 4) is examined next. p_s is observed regularly at the synoptic surface stations, and the North European station network is denser than the current network of GPS receivers. The p_s innovation data set is produced by the operational 33-km resolution operational HIRLAM NWP system run at the Finnish Meteorological Institute (FMI) for the period of October 2002 to September 2003. The model fits well the innovations in the autumn period (Fig. 2), and also in other seasons (not shown). The model for the ZHD term has a broad spatial scale with the e-folding distance of the order of 600 km.

As will be seen later, the ZHD term has a rather small contribution in eq. (4). This implies that the current NWP model background p_s is sufficiently accurate for the ZTD observation modelling. Note that the p_s innovation covariance in eq. (4) is multiplied by the factor a^2.

3.3. Integrated Water Vapour innovation covariance

Atmospheric humidity profiles are routinely measured by the radiosonde network. These profiles can be integrated in vertical in order to obtain IWV observations. The corresponding IWV innovation data are produced by the 33-km resolution operational HIRLAM NWP system at the FMI for a 1-yr period from October 2002 to September 2003, i.e. the same model configuration and period as for the p_s data set. The radiosonde network is sparse compared to the synoptic and GPS receiver networks. Thus, in order to gather enough statistical material also for small station separation distances, a larger geographical area is chosen for IWV data than for ZTD and p_s data (whole of Europe versus Scandinavian region).

There are 22–28 regularly observing radiosonde station pairs in the horizontal separation bin of 100 km throughout the year, while for bins of 200 and 300 km the numbers of pairs are 76–84 and 100–117, respectively. This results in wide 95% confidence intervals of innovation covariance values at small separation distances r. The sparseness of the radiosonde observation network is a general limitation of the observation method.

Figure 3 illustrates the model of the IWV innovation covariance for the autumn period. Figure 3, and similar figures for other seasons (not shown), supports the following conclusions. First, with increasing separation distance r, the innovation covariance decreases slowly and the general appearance of the IWV innovation covariance model is quite flat as compared with the ZTD innovation covariance model. The e-folding distance varies between about 160 and 230 km for different seasons. Secondly, the IWV innovation covariance asymptotically approaches zero with increasing separation distance r. Beyond a separation distance of about 500 km, the IWV innovation covariance is practically zero for all seasons.

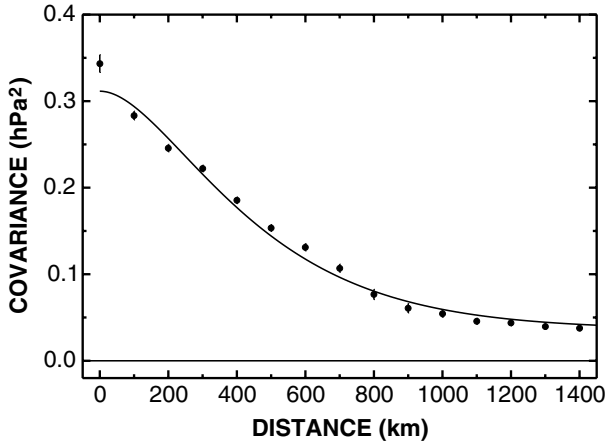

Fig 2. Synoptic p_s innovation covariance model for the three-month autumn period, i.e. an estimate of the ZHD term of eq. (4).

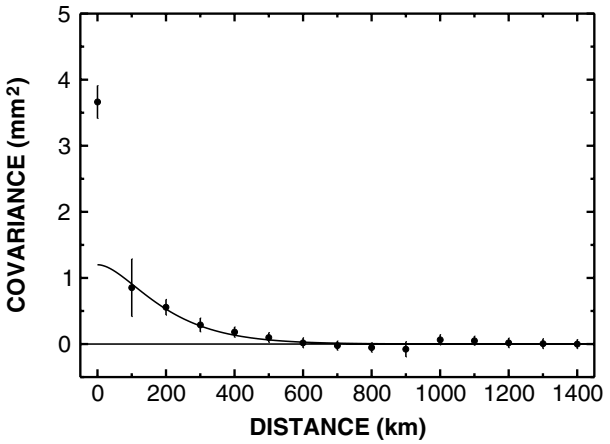

Fig 3. Radiosonde IWV innovation covariance model for the three-month autumn period, i.e. an estimate of the ZWD term of eq. (4).

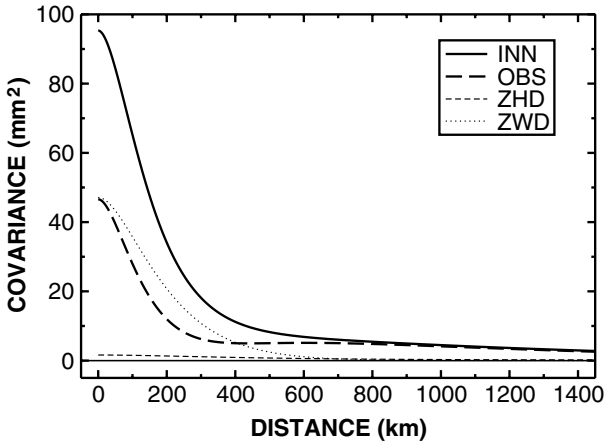

Fig 4. Terms of the GPS Zenith Delay Observation error covariance expression as estimated for the three-month autumn period. Terms INN, OBS, ZHD and ZWD refer to eq. (4).

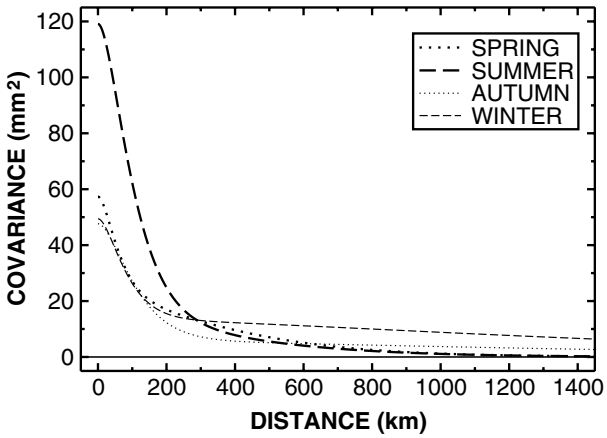

Fig 5. The $N = 2$ ZTD observation error covariance model (OBS model) for the three-month seasons as estimated in the model space.

4. Zenith Total Delay observation error covariance model

The $N = 2$ model for the OBS term is defined in this section first by 'estimation in model space' and then by 'estimation in innovation space'.

4.1. Estimation in model space

The $N = 2$ models for the three innovation terms of eq. (4) are displayed in Fig. 4, together with the $N = 6$ model for the OBS term, for the autumn period. This figure, and similar figures for other seasons (not shown), support the following conclusions. For small station separations, the OBS model (long-dashed line) decreases more rapidly with increasing separation distance than does the ZWD model (dotted line). However, for separation distances greater than about 500 km, the ZWD model is practically zero and the ZTD innovation covariance (the INN model, solid line) is mainly due to the OBS model. The contribution of the ZHD model (short-dashed line) is very small throughout the year. Note that the $N = 6$ model for the OBS model in Fig. 4 has a local minimum (maximum) at about 350 km (700 km) separation distance. This is, as explained in Section 2, due to the negative model parameter values. As a final step, the $N = 6$ model for the OBS term is reduced back to a $N = 2$ model.

The estimated $N = 2$ model parameter values for the standard three-month seasons and for the yearly mean are given in Table 1. The sum of R_1 and R_2 represents the magnitude of the OBS model at zero separation distance, and it is largest in summer (119 mm^2). For other seasons, the sum is only half the summer value. The length-scale parameter values (L_1 and L_2) also vary seasonally. L_1 oscillates smoothly between spring minimum and autumn maximum. The behaviour of L_2 values is different. The spring and summer values are around 200 km while the autumn and winter values are about 800 km.

Figure 5 visualizes the ZTD observation error covariance models of Table 1. For separation distances up to about 300 km, the summer curve (long-dashed line) has distinctly high values. For separation distances well over 300 km, the winter (short-dashed line) and autumn (thin dotted line) curves remain above zero due to broad-scale error covariance, in accordance with large values for L_2 in Table 1.

Table 1. The $N = 2$ model parameters for the ZTD observation error covariance model (OBS model) for the three-month seasons and for the yearly mean as estimated in the model space

	R_1 (mm^2)	L_1 (km)	R_2 (mm^2)	L_2 (km)
Spring	36.1	34.1	21.2	218
Summer	105	56.0	14.4	237
Autumn	41.9	61.0	5.71	813
Winter	36.1	46.1	13.3	833
Yearly mean	60.0	61.4	9.97	423

4.2. Estimation in innovation space

The ZTD observation error covariance model is defined here with the second approach (estimation in innovation space). The estimated parameter values for the three-month seasons and for the yearly mean are presented in Table 2. Comparison with Table 1 indicates a generally good agreement, in particular for the yearly mean values. The main differences in the covariance models appear at the shortest length-scales for seasonal values. The results of Table 2 are illustrated for the autumn period in Fig. 6. This figure, and similar figures for other seasons (not shown), suggests that the covariance model provides a good characterization of the residual bin-averaged covariance values of the OBS term. The 95% confidence interval is much wider in Fig. 6 for the 100-km separation distance bin than for other bins. Thus, the

Table 2. As Table 1, but as estimated in the innovation space

	R_1 (mm^2)	L_1 (km)	R_2 (mm^2)	L_2 (km)
Spring	90.6	23.0	22.5	214
Summer	175	34.8	28.7	168
Autumn	72.9	45.8	4.92	1730
Winter	29.2	55.5	12.5	870
Yearly mean	61.0	62.3	9.19	476

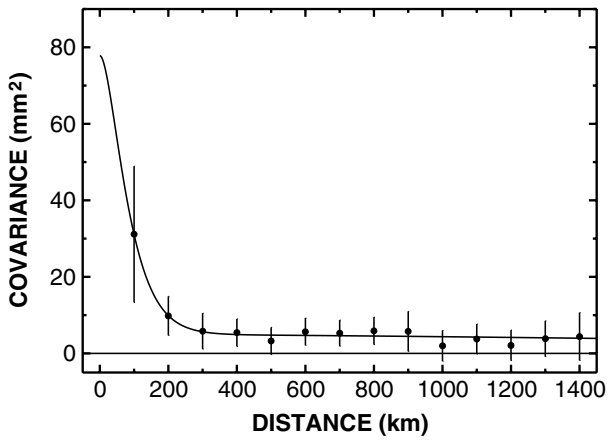

Fig 6. The $N = 2$ ZTD observation error covariance model (OBS model) for the three-month autumn period as estimated in the innovation space.

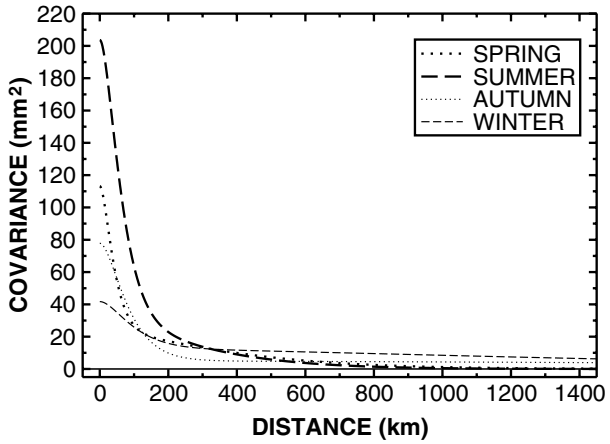

Fig 7. As Fig. 5. but as estimated in the innovation space.

shortest-scale structures of the OBS model should be interpreted cautiously.

Figure 7 displays the OBS model for all seasons. Results are qualitatively similar to those of Fig. 5, which used estimation in model space, and the conclusions are confirmed. The shortest-scale error covariance is largest in summer. The annual cycle of the observation error variance (covariance at zero separation) in Fig. 7 is clearer than in Fig. 5. The very broad-scale covariance structures (well over 300-km separation distances) for autumn and winter appear with both approaches. In general, the differences in the estimated ZTD observation error covariance using one or the other method appear mostly in the separation distances below 100 km. Slight differences can be seen in summer and autumn also for separation distances over 100 km. The shape of the modelled ZTD observation error covariance is also qualitatively similar with the spatial ZTD observation error correlation reported by Stoew (2004).

4.3. Estimated error standard deviations

The innovation variance (σ_d^2), i.e. innovation covariance at zero separation, consists of observation and background error variances (σ_o^2 and σ_b^2). The observation method (HL86; Daley, 1991; Bouttier and Courtier, 1999) enables estimation of the error standard deviations σ_o and σ_b for the observation types with uncorrelated errors.

In case of ZTD, the observation method only separates the uncorrelated observation error part, $\sigma_{o,u}$. Both σ_b and the correlated observation error, $\sigma_{o,c}$, contribute to the horizontal innovation covariance. These two contributions are separated here using the OBS model. These concepts are illustrated in Appendix B.

The estimated error standard deviations for the three-month seasons and for the yearly mean are given in Table 3. Generally speaking, for conventional observations with uncorrelated errors σ_o should remain constant, within the estimation uncertainty, throughout the year, while σ_b can vary from one season to another. This seems to be the case for σ_o of p_s, except for the rather low autumn value. For IWV σ_o, the seasonal variations are about ± 0.5 mm around the yearly mean value of 1.5 mm. These relatively large variations are indicative of estimation uncertainties. Background error covariance structures are short-scaled for humidity, and these scales are poorly sampled by the sparse radiosonde network.

ZTD σ_o varies by ± 2.2 mm around the yearly mean of 9.7 mm, i.e. relatively less than variations of IWV (Table 3). This is in accordance with the denser GPS receiver network. σ_o is

Table 3. The estimated observation and background error standard deviations

		Spring	Summer	Autumn	Winter	Year
p_s	σ_o (hPa)	0.29	0.29	0.18	0.35	0.31
	σ_b (hPa)	0.48	0.42	0.56	0.50	0.45
IWV	σ_o (mm)	1.4	2.2	1.6	1.1	1.5
	σ_b (mm)	0.99	1.4	1.1	0.81	0.95
ZTD	σ_o (mm)	8.1	11.6	9.1	7.2	9.7
	$\sigma_{o,c}$ (mm)	7.6	10.9	6.9	7.0	8.4
	$\sigma_{o,u}$ (mm)	2.8	3.8	5.9	1.4	4.9
	σ_b (mm)	6.2	9.0	6.9	5.1	6.0

dominated by the correlated part $\sigma_{o,c}$, especially in winter. $\sigma_{o,c}$ is related to the estimation errors in the geodetic network solution, and the statistical structure of these errors and hence $\sigma_{o,c}$ can vary from one season to another. $\sigma_{o,u}$, on the other hand, is related to receiver-dependent error sources such as instrumental random noise. For ZTD, it is $\sigma_{o,u}$ that might be thought of as a constant. Note that post-processed ZTD observations are used in this study. Accuracy of near-real-time observations would probably be worse.

The estimated σ_b for p_s has a minimum in summer, while for the humidity quantities, IWV and ZTD, there appears a maximum of σ_b in summer. The observed p_s appears to be more accurate than the background p_s, while the opposite is true for IWV and ZTD.

4.4. *Discussion on the accuracy of the results*

The innovation sequences used in this study are not homogeneous, but differ in time period, geographical area and NWP model background used in the innovation calculation. While the IWV innovation sequence is based on the radiosonde data from the whole of Europe, ZTD and p_s data only from the Scandinavian region are used. The ZTD innovation sequence is derived from a different HIRLAM implementation and from a different time period than the p_s and IWV innovation sequences. Innovation covariance includes the NWP background errors, which are specific to the model, time period and geographical area. These differences in the innovation sequences thus limit the accuracy of the results.

Two different implementations of the same algorithm are used in the covariance model parameter estimation with relatively similar results. This increases confidence in the robustness of the methods developed in this study. It is concluded therefore that the methodology itself is robust, but the accuracy of the results is limited by the innovation data.

5. Summary and discussion

In this paper, an estimation algorithm for the spatial GPS ZTD observation error covariance is developed. The error covariance is estimated as a linear combination of ZTD, p_s and IWV innovation covariances, respectively, using innovation sequences. The algorithm is a solution to a general limitation of the observation method to separate observation and background error contributions to the innovation covariance, in this particular case.

A generalized serial exponential covariance model is introduced and applied to model the ZTD observation error covariance. This model and the estimated model parameters can be implemented to data assimilation systems.

It is shown that the covariance model is not very sensitive to the implementation details of the algorithm. Differences appear, however, at very short separation distances (below 100 km) where radiosonde network data, and thus IWV innovation data, are sparse.

On short separation distances, the decrease of ZTD observation error covariance with increasing separation distance is steeper than the decrease of ZWD background error covariance. For separation distances more than about 500 km, the ZTD observation error covariance is close to the ZTD innovation covariance. In other words, IWV background error covariance is shorter-scaled than the ZTD observation error covariance. The ZHD background error covariance contributes little to the ZTD innovation covariance.

The estimated ZTD observation error covariance varies seasonally. For separation distances less than 300 km, the covariance is large in summer. For longer separation distances, i.e. for broad-scale error structures, non-zero error covariance is present in winter. The factors in the ZTD processing causing the observation error covariance seem to act in two scales. The relatively high covariance at separations smaller than 300 km may be related to the positioning errors that are common to closely located receivers in the network of stations. The broad-scale ZTD observation error covariance may be due to satellite orbit parameter errors and clock errors through the geodetic network solution.

The GPS slant delay observations (Ware et al., 1997; Alber et al., 2000) are meteorologically very interesting. Slant delays are processed for each satellite–receiver pair and their assimilation requires modelling of the refractivity field along the signal paths based on the NWP model data. One of the main advantages of the use of slant delays is that each receiver produces several observations at each time instant, and the number of useful slant delays is thus tenfold the number of zenith delays. Further research is needed for the development of models for the observation error covariance of slant delays. The methodology proposed in this paper is thought to be applicable for the zenith delays only.

The observation error covariance model is estimated by following the L-S fitting procedure. The M-L fitting procedure proposed by Dee and da Silva (1999) might as well be used for the estimation. The ‘ensemble assimilation method’ might provide an alternative framework for separating the observation and background errors, with the advantage of providing information in all scales resolved by the NWP model, not only in the scales resolved by the observation network.

6. Acknowledgments

This work is carried out within the EU FP5 project ‘TOUGH’. TOUGH is a shared-cost project (contract EVG1-CT-2002-00080) co-funded by the Research DG of the European Commission within the RTD activities of the Environment and Sustainable Development subprogramme (5th Framework Programme). Funding from TEKES, the National Technology Agency of Finland, is also thankfully acknowledged. The authors are grateful to Kalle Eerola (FMI) for providing the synoptic p_s and radiosonde IWV innovation data sets, and to Nils Gustafsson (SMHI) and

Jan Johansson (Onsala Observatory) for providing the GPS ZTD innovation data set.

7. Appendix A: Partitioning of zenith total delay innovation covariance

The difference between an observation y^{o} and an NWP model background y^{b}, i.e. innovation, can be written by introducing a hypothetical true value y^{t} as follows

$$d = y^{\mathrm{o}} - y^{\mathrm{b}} = y^{\mathrm{o}} - y^{\mathrm{b}} + y^{\mathrm{t}} - y^{\mathrm{t}} = \varepsilon^{\mathrm{o}} - \varepsilon^{\mathrm{b}},$$

where ε^{o} and ε^{b} are observation and background errors, respectively. The covariance of two innovation sequences from stations i and j is

$$\begin{aligned}\mathrm{cov}(d_i, d_j) &= \left\langle (\varepsilon_i^{\mathrm{o}} - \varepsilon_i^{\mathrm{b}}), (\varepsilon_j^{\mathrm{o}} - \varepsilon_j^{\mathrm{b}}) \right\rangle \\ &= \left\langle \varepsilon_i^{\mathrm{o}}, \varepsilon_j^{\mathrm{o}} \right\rangle - \left\langle \varepsilon_i^{\mathrm{o}}, \varepsilon_j^{\mathrm{b}} \right\rangle - \left\langle \varepsilon_i^{\mathrm{b}}, \varepsilon_j^{\mathrm{o}} \right\rangle + \left\langle \varepsilon_i^{\mathrm{b}}, \varepsilon_j^{\mathrm{b}} \right\rangle,\end{aligned}$$

where $\langle ., . \rangle$ is the expectation operator. If observation and background errors are uncorrelated, cross-covariance terms are zero and innovation covariance is a sum of observation and background error covariances.

The ZTD background value ($\mathrm{ZTD}^{\mathrm{b}}$) can be expressed by the NWP model surface pressure ($p_{\mathrm{s}}^{\mathrm{b}}$) and IWV ($\mathrm{IWV}^{\mathrm{b}}$) background values as follows

$$\mathrm{ZTD}^{\mathrm{b}} = a p_{\mathrm{s}}^{\mathrm{b}} + b\mathrm{IWV}^{\mathrm{b}},$$

where a and b are constants. The ZTD background error is then

$$\varepsilon_{\mathrm{ZTD}}^{\mathrm{b}} = a\varepsilon_{p_{\mathrm{s}}}^{\mathrm{b}} + b\varepsilon_{\mathrm{IWV}}^{\mathrm{b}}.$$

ZTD innovation can now be written as

$$d_{\mathrm{ZTD}} = \varepsilon_{\mathrm{ZTD}}^{\mathrm{o}} - \varepsilon_{\mathrm{ZTD}}^{\mathrm{b}} = \varepsilon_{\mathrm{ZTD}}^{\mathrm{o}} - a\varepsilon_{p_{\mathrm{s}}}^{\mathrm{b}} - b\varepsilon_{\mathrm{IWV}}^{\mathrm{b}}$$

and the ZTD innovation covariance between stations i and j is

$$\begin{aligned}\mathrm{cov}(d_{\mathrm{ZTD},i}, d_{\mathrm{ZTD},j}) = {} & \left\langle \varepsilon_{\mathrm{ZTD},i}^{\mathrm{o}}, \varepsilon_{\mathrm{ZTD},j}^{\mathrm{o}} \right\rangle - a \left\langle \varepsilon_{\mathrm{ZTD},i}^{\mathrm{o}}, \varepsilon_{p_{\mathrm{s}},j}^{\mathrm{b}} \right\rangle \\ & - b \left\langle \varepsilon_{\mathrm{ZTD},i}^{\mathrm{o}}, \varepsilon_{\mathrm{IWV},j}^{\mathrm{b}} \right\rangle - a \left\langle \varepsilon_{p_{\mathrm{s}},i}^{\mathrm{b}}, \varepsilon_{\mathrm{ZTD},j}^{\mathrm{o}} \right\rangle \\ & + a^2 \left\langle \varepsilon_{p_{\mathrm{s}},i}^{\mathrm{b}}, \varepsilon_{p_{\mathrm{s}},j}^{\mathrm{b}} \right\rangle + ab \left\langle \varepsilon_{p_{\mathrm{s}},i}^{\mathrm{b}}, \varepsilon_{\mathrm{IWV},j}^{\mathrm{b}} \right\rangle \\ & - b \left\langle \varepsilon_{\mathrm{IWV},i}^{\mathrm{b}}, \varepsilon_{\mathrm{ZTD},j}^{\mathrm{o}} \right\rangle + ab \left\langle \varepsilon_{\mathrm{IWV},i}^{\mathrm{b}}, \varepsilon_{p_{\mathrm{s}},j}^{\mathrm{b}} \right\rangle \\ & + b^2 \left\langle \varepsilon_{\mathrm{IWV},i}^{\mathrm{b}}, \varepsilon_{\mathrm{IWV},j}^{\mathrm{b}} \right\rangle.\end{aligned}$$

There are nine terms contributing to ZTD innovation covariance. Four cross-covariance terms between observation and background errors can be assumed zero. Two additional cross-covariance terms between p_{s} and IWV background errors are assumed zero. The ZTD innovation covariance is thus reduced to

$$\begin{aligned}\mathrm{cov}(d_{\mathrm{ZTD},i}, d_{\mathrm{ZTD},j}) = {} & \left\langle \varepsilon_{\mathrm{ZTD},i}^{\mathrm{o}}, \varepsilon_{\mathrm{ZTD},j}^{\mathrm{o}} \right\rangle + a^2 \left\langle \varepsilon_{p_{\mathrm{s}},i}^{\mathrm{b}}, \varepsilon_{p_{\mathrm{s}},j}^{\mathrm{b}} \right\rangle \\ & + b^2 \left\langle \varepsilon_{\mathrm{IWV},i}^{\mathrm{b}}, \varepsilon_{\mathrm{IWV},j}^{\mathrm{b}} \right\rangle.\end{aligned}$$

Finally, p_{s} and IWV background error covariances equal p_{s} and IWV innovation covariances for $i \neq j$ as observation errors of synoptic p_{s} and radiosonde IWV are not spatially correlated, i.e.

$$\left\langle \varepsilon_{p_{\mathrm{s}},i}^{\mathrm{b}}, \varepsilon_{p_{\mathrm{s}},j}^{\mathrm{b}} \right\rangle = \left\langle d_{p_{\mathrm{s}},i}, d_{p_{\mathrm{s}},j} \right\rangle$$

and

$$\left\langle \varepsilon_{\mathrm{IWV},i}^{\mathrm{b}}, \varepsilon_{\mathrm{IWV},j}^{\mathrm{b}} \right\rangle = \left\langle d_{\mathrm{IWV},i}, d_{\mathrm{IWV},j} \right\rangle,$$

for $i \neq j$ and thus

$$\begin{aligned}\mathrm{cov}(d_{\mathrm{ZTD},i}, d_{\mathrm{ZTD},j}) = {} & \mathrm{cov}(\varepsilon_{\mathrm{ZTD},i}^{\mathrm{o}}, \varepsilon_{\mathrm{ZTD},j}^{\mathrm{o}}) \\ & + a^2 \mathrm{cov}(d_{p_{\mathrm{s}},i}, d_{p_{\mathrm{s}},j}) \\ & + b^2 \mathrm{cov}(d_{\mathrm{IWV},i}, d_{\mathrm{IWV},j}).\end{aligned} \tag{A1}$$

The ZTD observation error covariance can now be estimated using ZTD innovation covariance estimated from ground-based GPS receivers, p_{s} innovation covariance estimated from synoptic stations, and IWV innovation covariance estimated from the radiosonde network.

8. Appendix B: Estimation of the error standard deviations

The observation method (HL86) allows estimation of the error variances for observation types with uncorrelated errors. The innovation covariance model (solid line in Fig. 8), which is a function of station separation r, is L-S fitted to the bin-averaged innovation covariances (dots). Because the observation errors are uncorrelated, the innovation variance σ_{d}^2 can be separated into background (σ_{b}^2) and observation (σ_{o}^2) error variance contributions.

In the general case of correlated observation errors, the uncorrelated part of the observation error variance ($\sigma_{\mathrm{o,u}}^2$ in Fig. 9) can still be separated from σ_{d}^2 by the observation method. However, it provides no way to further separate the spatially correlated error part (solid line) into contributions from the background error (dashed line) and from the correlated part of the observation error ($\sigma_{\mathrm{o,c}}^2$), without additional information.

The proposed algorithm first estimates the spatially correlated error contribution to σ_{d}^2, i.e. $\sigma_{\mathrm{b}}^2 + \sigma_{\mathrm{o,c}}^2$, by the observation method. The estimated ZTD observation error covariance model

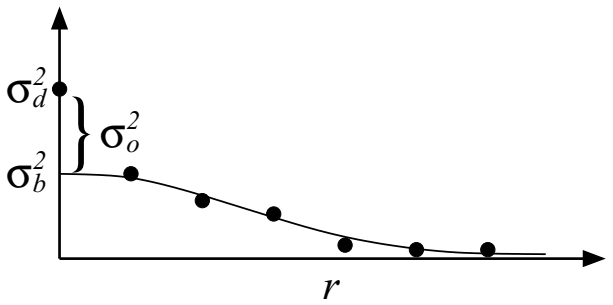

Fig 8. Separation of innovation covariance into its components in a special case of uncorrelated observation errors.

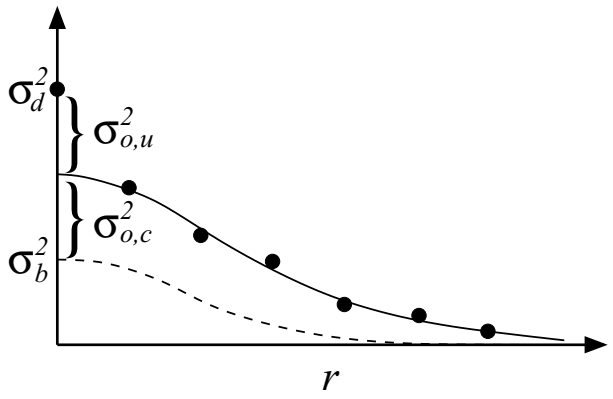

Fig 9. Separation of innovation covariance into its components in a general case of spatially correlated observation errors.

at zero separation equals to $\sigma^2_{\mathrm{o,c}}$, and with this additional information σ^2_{b} and $\sigma^2_{\mathrm{o,c}}$ can be separated. The variance of the total observation error is then $\sigma^2_{\mathrm{o}} = \sigma^2_{\mathrm{o,u}} + \sigma^2_{\mathrm{o,c}}$. The error standard deviations (σ_{o}, $\sigma_{\mathrm{o,u}}$, $\sigma_{\mathrm{o,c}}$, σ_{b}) are square roots of the corresponding error variances.

References

Alber, C., Ware, R., Rocken, C. and Braun, J. 2000. Obtaining single path phase delays from GPS double differences. *Geophys. Res. Lett.* **27**, 2661–2664.

Bevis, M., Businger, S., Herring, T., Rocken, C., Anthes, R. et al. 1992. GPS meteorology: remote sensing of atmospheric water vapor using the Global Positioning System. *J. Geophys. Res.* **97**, 15 787–15 801.

Bormann, N., Saarinen, S., Kelly, G. and Thépaut, J.-N. 2003. The spatial structure of observation error in atmospheric motion vectors from geostationary satellite data. *Mon. Wea. Rev.* **131**, 706–718.

Bouttier, F. and Courtier, P. 1999. Data assimilation concepts and methods. ECMWF meteorological training course lecture notes. 58 pp. Available from ECMWF, Shinfield Park, Reading, RG2 9AX, UK.

Daley, R. 1991. *Atmospheric Data Analysis*. Cambridge Atmospheric and Space Science Series. Cambridge University Press, Cambridge, 457 pp.

De Pondeca, M. and Zou, X. 2001. A case study of the variational assimilation of GPS zenith delay observations into a mesoscale model. *J. Appl. Meteorol.* **40**, 1559–1576.

Dee, D. P. and da Silva, A. M. 1999. Maximum-likelihood estimation of forecast and observation error covariance parameters. Part I: methodology. *Mon. Wea. Rev.* **127**, 1822–1834.

Dee, D. P., Gaspari, G., Redder, C., Rukhovets, L. and da Silva, A. M. 1999. Maximum-likelihood estimation of forecast and observation error covariance parameters. Part II: applications. *Mon. Wea. Rev.* **127**, 1835–1849.

Gustafsson, N. 2002. Assimilation of ground-based GPS data in HIRLAM 3D-Var. Proceedings of the HIRLAM Workshop on Variational Data Assimilation and Remote Sensing, Finnish Meteorological Institute, Helsinki 21–23 Jan 2002. 89–96. Available from the HIRLAM Project, c/o Per Undén, SMHI, S-60176 Norrköping, Sweden.

Gustafsson, N., Berre, L., Hörnquist, S., Huang, X.-Y., Lindskog, M. et al. 2001. Three-dimensional variational data assimilation for a limited area model. Part I: general formulation and the background error constraint. *Tellus* **53A**, 425–446.

Haase, J., Ge, M., Vedel, H. and Calais, E. 2003. Accuracy and variability of GPS tropospheric delay measurements of water vapor in the Western Mediterranean. *J. Appl. Meteorol.* **42**, 1547–1568.

Hollingsworth, A. and Lönnberg, P. 1986. The statistical structure of short-range forecast errors as determined from radiosonde data. Part I: the wind field. *Tellus* **38A**, 111–136 (HL86).

Järvinen, H., Andersson, E. and Bouttier, F. 1999. Variational assimilation of time sequences of surface observations with serially correlated errors. *Tellus* **51A**, 469–488.

Lindskog, M., Gustafsson, N., Navascués, B., Mogensen, K. S., Huang, X.-Y. et al. 2001. Three-dimensional variational data assimilation for a limited area model. Part II: observation handling and assimilation experiments. *Tellus* **53A**, 447–468.

McClatchey, R. A., Fenn, R. W., Selby, J. E. A., Volz, F. E. and Garing, J. S. 1971. Optical properties of the atmosphere. Report AFCRL-71-0279, Air Force Cambridge Research Laboratories. 85 pp. Available from Air Force Geophysics Laboratory, Hanscom Air Force Base, MA 01731, USA.

Saastamoinen, J. 1972. Atmospheric correction for the troposphere and stratosphere in radio ranging of satellites. In: *The Use of Artificial Satellites for Geodesy, Geophysics Monograph Series* **Vol. 15** (eds S. W. Henriksen, A. Mancini, and B. H. Chovitz). AGU, Washington, DC, 247–251.

Stoew, B. 2004. Description and analysis of data and errors in GPS meteorology. Technical report No. 469. Chalmers University of Technology, 90 pp.

Thiébaux, H. 1985. On approximations to geopotential and wind-field correlation structures. *Tellus* **37A**, 126–131.

Undén, P., Rontu, L., Järvinen, H., Lynch, P., Calvo, J. et al. 2002. HIRLAM-5 Scientific Documentation. 144 pp. Available from Hirlam-5 Project, c/o Per Undén, SMHI, S-60176, Norrköping, Sweden.

Ware, R., Alber, C., Rocken, C. and Solheim, F. 1997. Sensing integrated water vapor along GPS ray paths. *Geophys. Res. Lett.* **24**, 417–420.